

Discovery, Synthesis, and Pharmacological Evaluation of Spiropiperidine Hydroxamic Acid Based Derivatives as Structurally Novel Histone Deacetylase (HDAC) Inhibitors

Mario Varasi,^{†,‡} Florian Thaler,^{*,§,‡} Agnese Abate,^{†,‡} Chiara Bigogno,^{||} Roberto Boggio,[§] Giacomo Carezzi,^{†,‡} Tiziana Cataudella,[†] Roberto Dal Zuffo,[§] Maria Carmela Fulco,^{†,‡} Marco Giulio Rozio,^{||} Antonello Mai,[⊥] Giulio Dondio,^{||} Saverio Minucci,^{‡,#} and Ciro Mercurio[†]

[†]Genextra Group, DAC SRL, Via Adamello 16, 20139 Milan, Italy

[‡]European Institute of Oncology, Via Adamello 16, 20139 Milan, Italy

[§]Genextra Group, Congenia SRL, Via Adamello 16, 20139 Milan, Italy

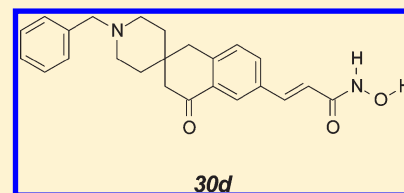
^{||}NiKem Research SRL, Via Zambelletti 25, 20021 Baranzate (MI), Italy

[⊥]Dipartimento di Chimica e Tecnologie del Farmaco, Istituto Pasteur-Fondazione Cenci Bolognetti, Università degli Studi di Roma "La Sapienza", P.le A. Moro 5, 00185 Roma, Italy

[#]Department of Biomolecular Sciences and Biotechnologies, University of Milan, Via Celoria, 26, 20133 Milan, Italy

S Supporting Information

ABSTRACT: New spiro[chromane-2,4'-piperidine] and spiro[benzofuran-2,4'-piperidine] hydroxamic acid derivatives as HDAC inhibitors have been identified by combining privileged structures with a hydroxamic acid moiety as zinc binding group. The compounds were evaluated for their ability to inhibit nuclear extract HDACs and for their in vitro anti-proliferative activity on different tumor cell lines. This work resulted in the discovery of spirocycle **30d** that shows good oral bioavailability and tumor growth inhibition in an HCT-116 murine xenograft model.



INTRODUCTION

Chemical modifications of DNA and histones play an essential role for modulating transcription processes in eukaryotic cells. Histone acetylation leads to the relaxation of chromatin and thus generally to gene activation. Conversely, hypoacetylation causes chromatin condensation resulting predominantly in transcriptional repression.^{1,2} The acetylation status is mediated by two enzyme families, histone acetyl transferases (HATs) and histone deacetylases (HDACs). The HDAC family can be classified into two groups: the "classical" HDACs, which are zinc-dependent amidohydrolases (classes I, II, and IV), and the NAD⁺ dependent sirtuins (class III). Class I HDACs comprise HDACs 1–3 and HDAC 8. They are predominantly nuclear enzymes and are ubiquitously expressed, whereas class II HDACs (HDACs 4–7, 9, and 10) are found in the nucleus and in the cytosol.^{3,4} HDAC 11 is the sole member of class IV HDACs. Perturbations of the acetylation level are associated with aberrant transcriptional activity, and HDACs have been identified as attractive targets for cancer therapy. Indeed, even though the exact mechanism of HDAC inhibitors as anticancer agents has not been fully elucidated, several compounds have demonstrated potent antitumoral activity in preclinical and clinical studies by increasing the acetylation status of histones and non-histones and inducing transcriptional events involved in growth arrest, differentiation, and apoptotic cell death.^{5–11} The hydroxamic acid derivative

SAHA **1**^{12,13} (also known as vorinostat) and the cyclic depsipeptide romidepsin or FK228 **2**¹⁴ are the first two compounds to gain market authorization: both HDAC inhibitors have been approved by the FDA for the treatment of cutaneous T-cell lymphoma (CTCL). Other compounds in clinical trials for the treatment of hematological and solid tumors include the hydroxamic acids panobinostat or LBH589 **3** (Novartis, phase III),¹⁵ PXD101 or belinostat **4** (Topotarget, phase III),¹⁶ SB-939 **5** (S*Bio, phase II),¹⁷ the benzamides SNDX-275 or MS-275 **6** (Syndax, phase II),¹⁸ and MGCD-0103 **7** (methylgene, phase II)¹⁹ (Figure 1).

We have recently described the synthesis and the biological activity of phenyloxopropenyl and amidopropenyl hydroxamic acid derivatives^{20,21} as potent inhibitors of HDACs. The compounds, comparable to the most advanced hydroxamic acid HDAC inhibitors in clinical studies, such as **1**, **3**, and **4**, exhibited an oral bioavailability of less than 20% in mice. Therefore, we explored new chemical entities with a (potential) superior oral bioavailability. Privileged structures with their inherent affinity for diverse biological targets represent an ideal source of core scaffolds for the design of molecules able to target various receptors.^{22–24} Conformationally constrained

Received: February 9, 2011

Published: March 21, 2011

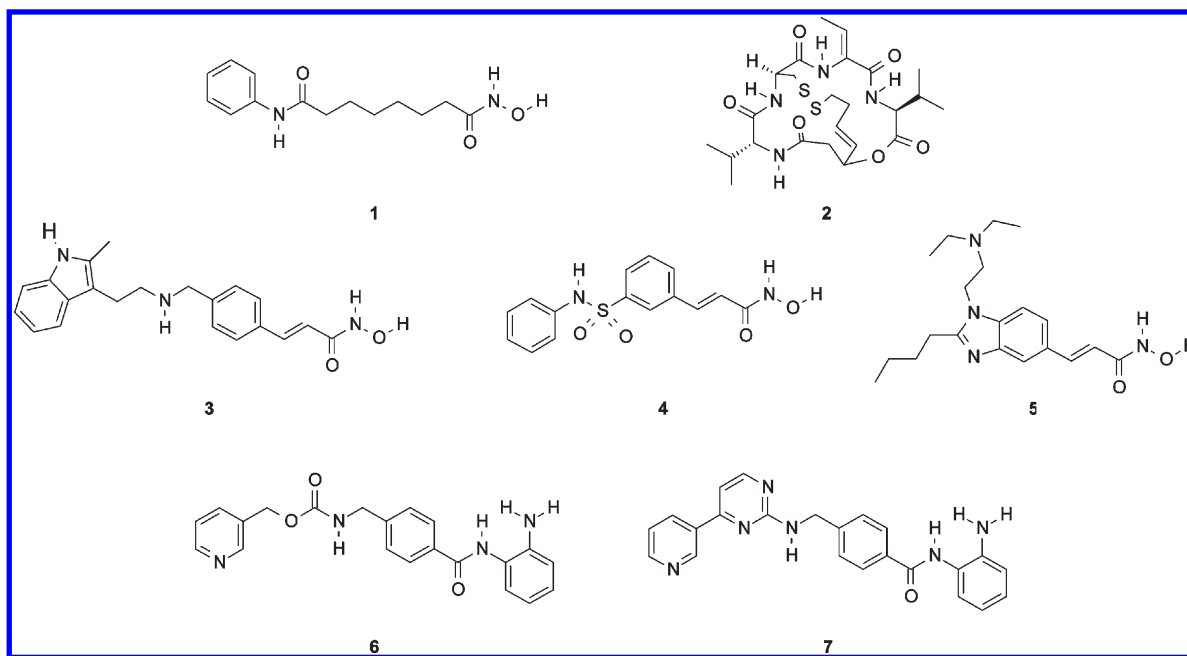
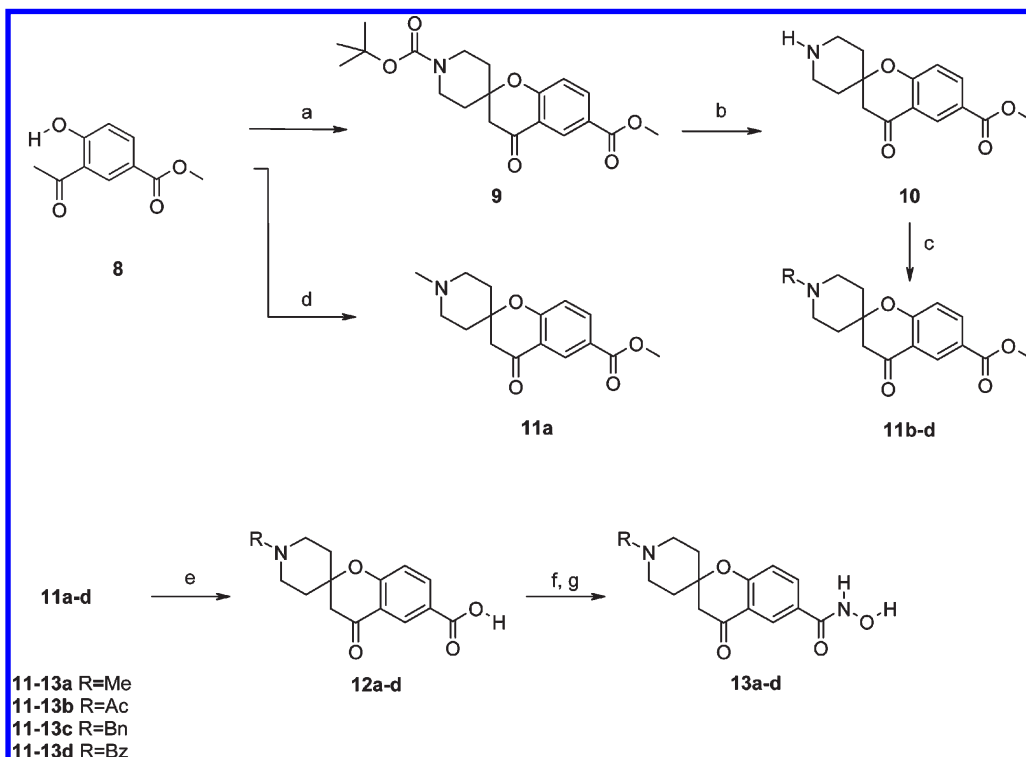


Figure 1. HDAC inhibitors in clinical development with compounds 1 and 2 having marketing approval for the treatment of cutaneous T-cell lymphoma (CTCL).

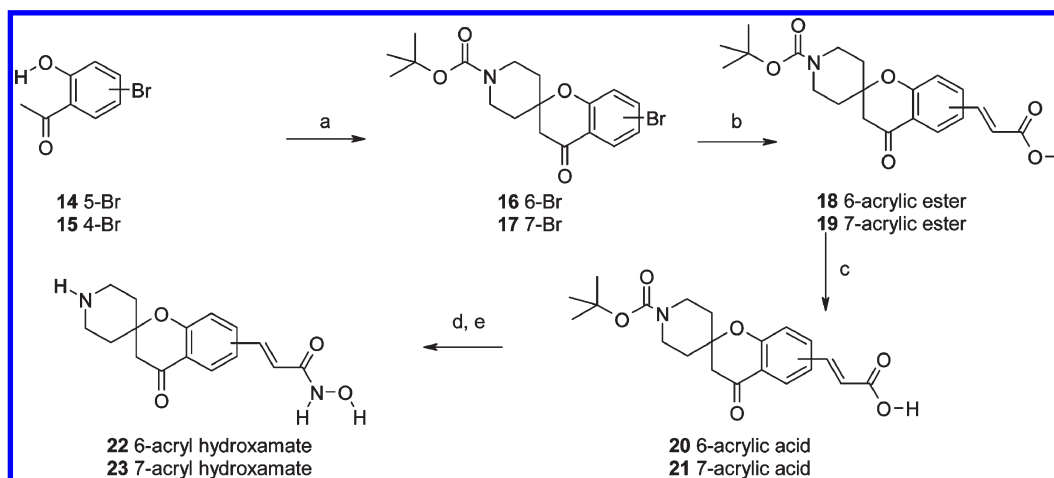
Scheme 1^a



^a Reagents and conditions: (a) MeOH, *N*-BOC-piperidin-4-one, pyrrolidine, reflux; (b) HCl, dioxane, room temp; (c) CH₂Cl₂, TEA; R-Br or R-Cl, room temp; (d) MeOH, *N*-Me-piperidin-4-one, pyrrolidine, reflux; (e) MeOH/H₂O, NaOH, 50 °C; (f) CH₂Cl₂, EDC, HOBT, NH₂OTHP, room temp; (g) CH₂Cl₂, Et₂O, HCl, room temp.

4-oxospiro[chroman-2,4'-piperidine] ring systems are privileged structures in the terminology of Evans et al.²⁵ the reduced molecular flexibility, the small size, and polarity present favorable

physical properties for oral bioavailability. The spirochromane moiety is present in structures acting as antiarrhythmic agents,²⁶ α_{1a}-receptor antagonists,²⁷ inhibitors of histamine release,²⁸

Scheme 2^a

^a Reagents and conditions: (a) MeOH, *N*-BOC-piperidin-4-one, pyrrolidine, reflux; (b) DMF, TEA, Pd(OAc)₂, PPh₃, methyl acrylate, 100 °C; (c) MeOH/H₂O, NaOH, 50 °C; (d) CH₂Cl₂, EDC, HOBt, NH₂OTHP, room temp; (e) CH₂Cl₂, dioxane, HCl, room temp.

growth hormone secretagogues,²⁹ dementia alleviating agents,³⁰ δ -opioid receptor ligands,^{31,32} stearoyl-CoA desaturase 1 inhibitors,^{33,34} acetyl-CoA carboxylase inhibitors,³⁵ or antiproliferative agents.³⁶ In the present study, we describe the synthesis and biological characterization of spiro[chromane-2,4'-piperidine] and spiro[benzofuran-2,4'-piperidine] combined with a hydroxamic acid moiety as zinc binding group to give derivatives with HDAC inhibitory activity.

CHEMISTRY

The *N*-hydroxy-spiro[chromane-2,4'-piperidine]-6-yl} carboxamides 13a–d were prepared starting from 3-acetyl-4-hydroxybenzoic acid methyl ester (8),³⁷ as illustrated in Scheme 1. Reaction of 8 with 1-(*tert*-butyloxycarbonyl)piperidine-4-one (*N*-BOC-piperidin-4-one) or 1-methylpiperidin-4-one in the presence of pyrrolidine gave the spirocyclic methyl ester 9 or 11a. Treatment of 9 with hydrogen chloride (HCl) in dioxane led to the free amine 10, which was then further functionalized either by alkylation with benzyl bromide or by acylation with acetyl or benzoyl chloride, giving intermediates 11b–d. Saponification of the methyl esters 11a–d with sodium hydroxide (NaOH) gave the carboxylic acids 12a–d, which were coupled with NH₂OTHP (*O*-(tetrahydropyran-2-yl)hydroxylamine) in the presence of EDC (*N*-(3-dimethylaminopropyl)-*N'*-ethylcarbodiimide hydrochloride) and HOBt (*N*-hydroxybenzotriazole). Cleavage of the protecting group with hydrogen chloride (HCl) in diethyl ether afforded the hydroxamates 13a–d.

(*E*)-*N*-Hydroxy-3-{4-oxospiro[chromane-2,4'-piperidine]-6-yl}acrylamide (22) and the spiro[chromane-2,4'-piperidine]-7-yl derivative 23 were prepared as shown in Scheme 2. Reaction of the commercially available 1-(5-bromo-2-hydroxyphenyl)ethanone (14) and 1-(4-bromo-2-hydroxyphenyl)ethanone (15)³⁸ with *N*-BOC piperidin-4-one was carried out according to the procedure described above in Scheme 1. The obtained spirocyclic methyl esters 16 and 17 were then submitted to the Heck reaction with methyl acrylate in the presence of palladium acetate [Pd(OAc)₂], PPh₃, and triethylamine (TEA) in DMF, affording the spirocyclic methyl esters 18 and 19. Hydrolysis of the methyl ester with NaOH and subsequent conversion to the hydroxamic acid following the procedure

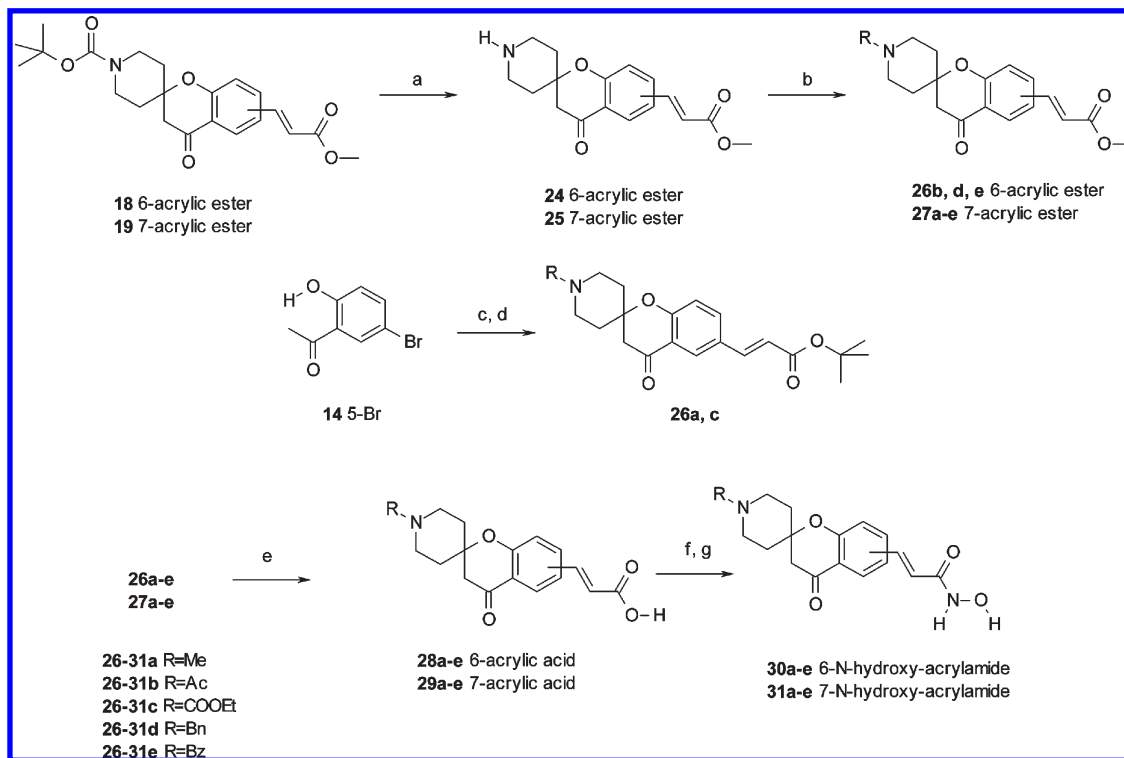
described above for compounds 13a–d (Scheme 1) furnished the *N*-hydroxyspiro[chromane-2,4'-piperidine]acrylamides 22 and 23.

N-Substituted spiro[chromane-2,4'-piperidine]acrylhydroxamates 30a–e and 31a–e were prepared as exemplified in Scheme 3. The BOC protection groups of the acrylic acid methyl esters 18 and 19 were cleaved in acidic conditions, giving the free amines 24 and 25, which were then functionalized through alkylation, reductive amination, or acylation to afford 26b, 26d, 26e, and 27a–e. The *tert*-butyl esters 26a and 26c were obtained by spirocyclization of 14 with 1-methylpiperidin-4-one or 1-ethylloxycarbonylpiperidin-4-one and subsequent Heck reaction with *tert*-butyl acrylate. Cleavage of methyl ester with NaOH and the *tert*-butyl ester with trifluoroacetic acid (TFA) gave the carboxylic acids, which were then coupled with NH₂OTHP utilizing EDC and HOBt. Acidic deprotection of tetrahydropyranyl moiety afforded the desired hydroxamic acids 30a–e and 31a–e.

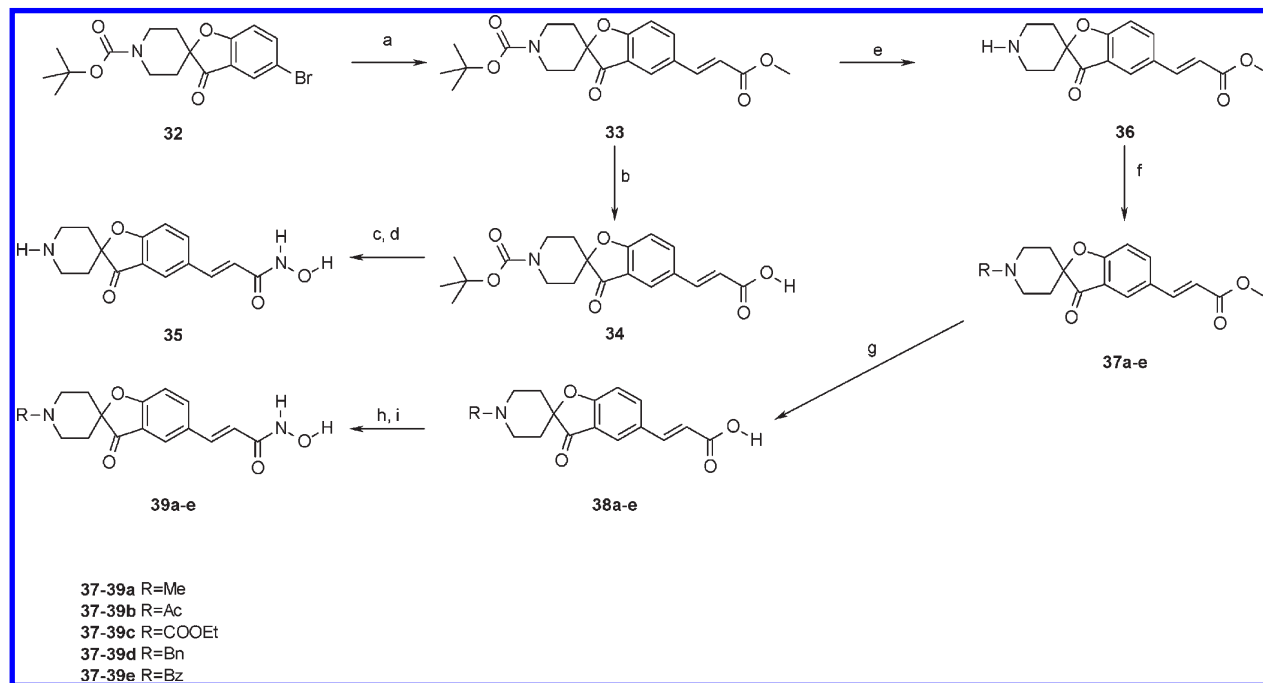
(*E*)-*N*-Hydroxy-3-{3-oxospiro[benzofuran-2(3H),4'-piperidin]-5-yl}acrylamide (35) was synthesized as described in Scheme 4. The spirobenzofuran 32³⁹ was coupled with methyl acrylate following the procedures outlined in Scheme 2 for the acrylic esters 18 and 19. Basic hydrolysis of the methyl ester afforded the acrylic acid 34, which was then subsequently converted into the desired hydroxamic acid according to Scheme 1.

N-Substituted spirobenzofuran acrylhydroxamates 39a–e were prepared starting from the BOC protected spiro[benzofuran-2(3H)-4'-piperidin]acrylic acid methyl ester 33 (Scheme 4). Deprotection of the BOC group gave the free amine 36, which was then either alkylated with benzyl bromide or acylated with acetyl chloride, benzoyl chloride, or ethyl chloroformate in presence of TEA. Reductive amination with formaldehyde in the presence of sodium triacetoxyborohydride [NaBH(OAc)₃] as reducing agent gave the *N*-methyl intermediate 37a. Hydrolysis of the methyl esters followed by EDC coupling with NH₂OTHP and final cleavage of the tetrahydropyranyl protecting group furnished the hydroxamic acid derivatives 39a–e.

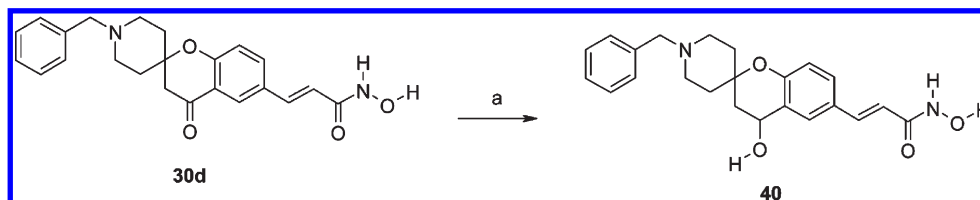
(*E*)-*N*-Hydroxy-3-{1'-benzyl-4-hydroxyspiro[chromane-2,4'-piperidine]-6-yl}acrylamide (40) was prepared by reducing the corresponding oxospiropiperidine derivative 30d with sodium borohydride (NaBH₄) as outlined in Scheme 5.

Scheme 3^a

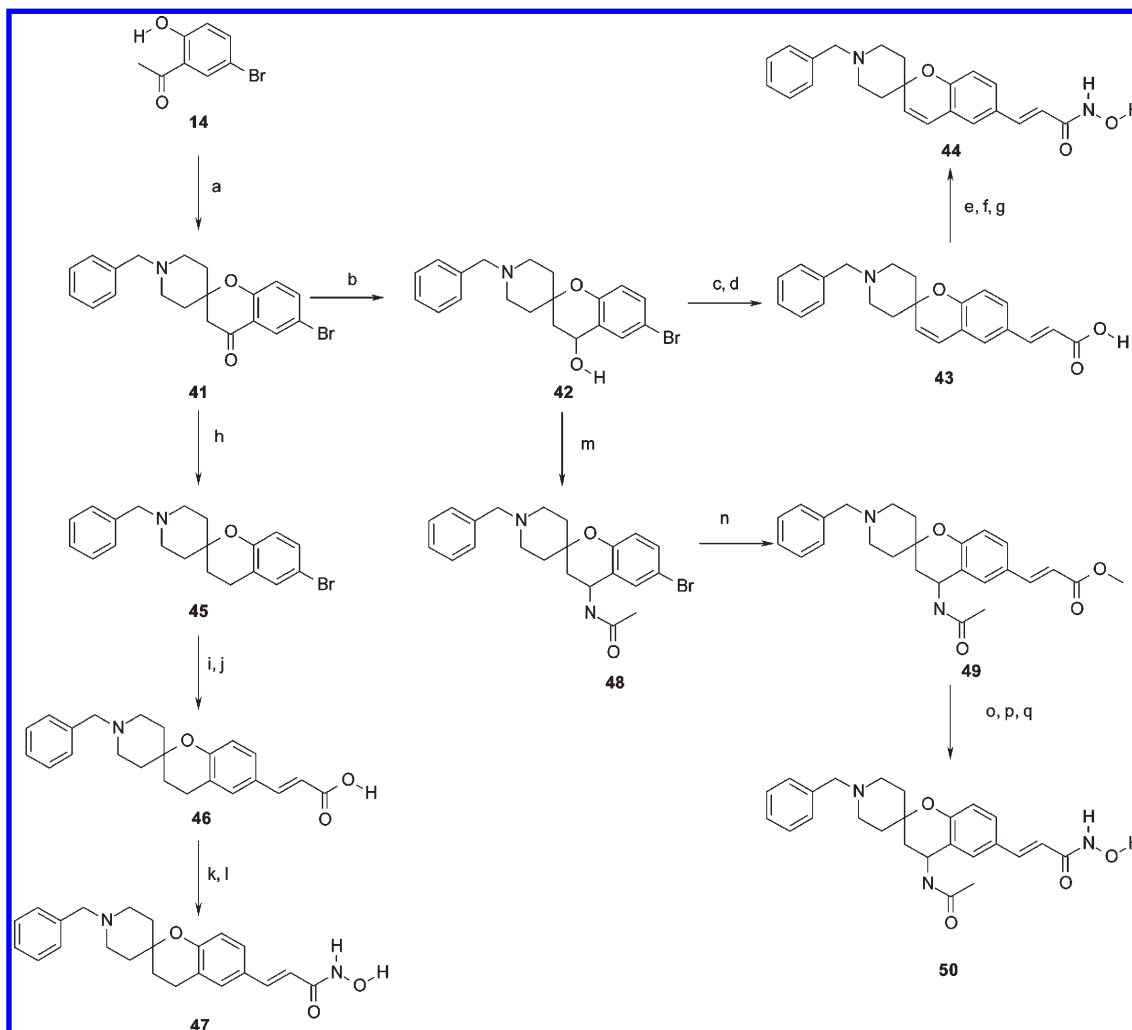
^a Reagents and conditions: (a) CH₂Cl₂, dioxane, HCl, room temp; (b) CH₂Cl₂, TEA, R-Br or R-Cl, room temp or for 27a CH₂Cl₂, HCHO, NaBH(Ac)₃, room temp; (c) MeOH, *N*-Me-piperidin-4-one or *N*-ethyloxycarbonyl-piperidin-4-one, pyrrolidine, reflux; (d) DMF, TEA, Pd(OAc)₂, *tert*-butyl acrylate, 100 °C; (e) MeOH/H₂O, NaOH, 50 °C or for 27a dioxane/water, NaOH, room temp or for 26a and 26c CH₂Cl₂, TFA, room temp; (f) CH₂Cl₂, EDC, HOBT, NH₂OTHP, room temp; (g) CH₂Cl₂, dioxane or Et₂O, HCl, room temp.

Scheme 4^a

^a Reagents and conditions: (a) DMF, TEA, Pd(OAc)₂, PPh₃, methyl acrylate, 100 °C; (b, g) MeOH/H₂O, NaOH, 50 °C; (c, h) CH₂Cl₂, EDC, HOBT, NH₂OTHP, room temp; (d, i) CH₂Cl₂, Et₂O, HCl, room temp; (e) HCl, dioxane, room temp; (f) CH₂Cl₂, TEA, R-Br or R-Cl, room temp or for 37a CH₂Cl₂, HCHO, NaBH(Ac)₃, room temp.

Scheme 5^a

^a Reagents and conditions: (a) MeOH, NaBH₄, room temp.

Scheme 6^a

^a Reagents and conditions: (a) MeOH, *N*-Bn-piperidin-4-one, pyrrolidine, reflux; (b) MeOH, NaBH₄, room temp; (c, i, n) DMF, TEA, Pd(OAc)₂, PPh₃, methyl acrylate, 100 °C; (d) THF, *p*-TsOH, reflux; (e, j, o) MeOH/H₂O, NaOH, 50 °C; (f, k, p) CH₂Cl₂, EDC, HOBT, NH₂OTHP, room temp; (g, l, q) CH₂Cl₂, dioxane, HCl, room temp; (h) EtOH, Zn, HCl, room temp; (m) CH₃CN, H₂SO₄, -10 to 0 °C, then room temp.

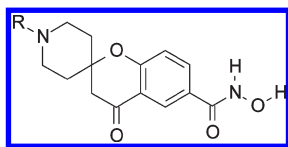
The benzylspiro-piperidine compounds **44**, **47**, and **50** were prepared as illustrated in Scheme 6. Condensation of 1-(5-bromo-2-hydroxyphenyl)ethanone (**14**) with *N*-benzylpiperidin-4-one in the presence of pyrrolidine gave the spiro-piperidine **41**. Reduction of the carbonyl group with NaBH₄ furnished intermediate **42**. Heck reaction with methyl acrylate in the presence of Pd(OAc)₂, PPh₃, and TEA and subsequent elimination of the alcohol gave the spirochromene methyl ester **43**. Conversion of the methyl ester into the hydroxamic acid **44** was achieved following the procedures

described in Scheme 2. Reduction of the oxspiropiperidine **41** with zinc in HCl furnished the spirochromane **45**. Heck reaction with methyl acrylate and subsequent saponification of the ester gave the acrylic acid **46**. EDC coupling with NH₂OTHP and final cleavage of the tetrahydropyranyl protecting group with HCl in dioxane afforded the requisite hydroxamic acid **47**. Ritter reaction of **42** with acetonitrile and sulfuric acid led to acetylaminospiro-piperidine **48**, which was then converted into the desired *N*-hydroxyacrylamide **50** as described for compound **47**.

BIOLOGY

The HDAC inhibitory activity of the synthesized spiro-piperidine derivatives was measured using a commercially available

Table 1. HDAC Enzyme and Antiproliferative Activity Data for Spiro[chromane-2,4'-piperidine]-6-yl]-*N*-hydroxybenzamide 13a–d^a



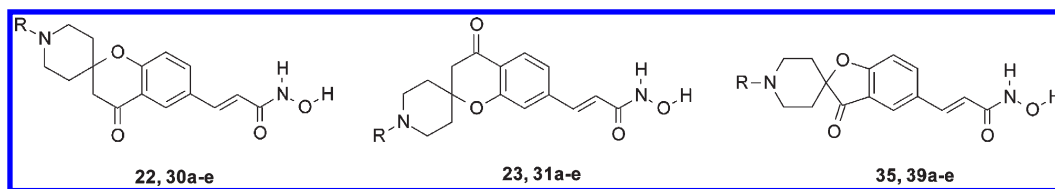
R	activity (μM)			
	HDAC	K562	A549	HCT-116
13a	CH ₃	>50	>50	>50
13b	acetyl	>50	>50	>50
13c	benzyl	24	16	22
13d	benzoyl	29	>50	>50

^a Assays done in replicates ($n \geq 2$). Mean values are shown, and the standard deviations are <30% of the mean.

HDAC assay kit, with partially purified HeLa nuclear extracts as the source for HDACs and a fluorogenic acetylated histone peptide fragment (Fluor de Lys) as the substrate. In addition to these biochemical experiments, we also investigated the ability of these compounds to inhibit cancer cell growth using the human chronic myelogenous leukemia cell line K562, carcinomic human alveolar basal epithelial cells A549, and human colon cancer cells HCT-116. HDAC inhibitory data and cellular activity of the compounds are compiled in Tables 1–3. As shown in Table 1, the methyl and the acetyl derivatives 13a and 13b were virtually inactive in the enzymatic assay, whereas the benzyl and the benzoyl analogues 13c and 13d exhibited IC₅₀ of 24 and 29 μM , respectively. Compound 13c showed inhibitory activities with IC₅₀ of around 20 μM for all three cell lines in the antiproliferative assay, whereas the three other compounds had IC₅₀ exceeding 50 μM .

Recently we reported about hydroxamic acid derivatives having minimum structural requirements for HDAC inhibition.²⁰ We had found that *N*-hydroxybenzamide showed a modest HDAC inhibitory activity. Introduction of an acrylic group resulted in a substantial increase of activity: *N*-hydroxycinnamide inhibited 55% of the HDAC enzyme activity at 1 μM .²⁰ These results stimulated the synthesis of new spiro-piperidine acrylydroxamate derivatives with the goal to obtain compounds with an increased biochemical and cellular activity. The first series

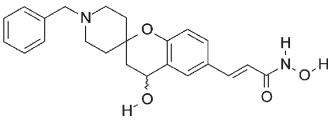
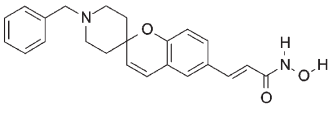
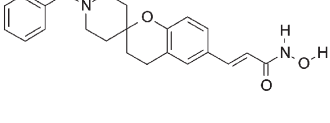
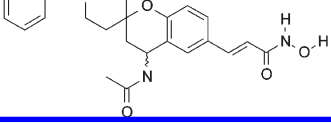
Table 2. HDAC Enzyme and Antiproliferative Activity Data for Spiro[chromane-2,4'-piperidine] and Spiro[benzofuran-2(3*H*)-4'-piperidin]-*N*-hydroxyacrylamides 22, 23, 30a–e, 31a–e, 35, and 39a–e^a



R	activity (μM)				
	HDAC	K562	A549	HCT-116	
22	H	0.082	5.77	2.72	1.59
30a	CH ₃	0.288	0.806	1.04	0.266
30b	acetyl	0.641	9.37	26.2	5.66
30c	ethyloxycarbonyl	0.140	2.08	5.27	2.14
30d	benzyl	0.121	0.399	0.773	0.477
30e	benzoyl	0.316	1.65	5.52	2.20
23	H	1.41	>50	24.8	35.5
31a	CH ₃	5.84	4.50	3.76	5.72
31b	acetyl	1.04	6.08	11.3	36.0
31c	ethyloxycarbonyl	0.408	2.19	2.78	3.03
31d	benzyl	2.173	8.94	12.2	8.41
31e	benzoyl	0.366	3.19	8.78	4.92
35	H	0.221	1.69	1.09	0.832
39a	CH ₃	0.538	0.397	1.07	0.337
39b	acetyl	>50	>50	>50	>50
39c	ethyloxycarbonyl	2.99	2.61	20.2	11.8
39d	benzyl	0.932	4.11	5.94	3.10
39e	benzoyl	2.55	7.43	22.1	12.3

^a Assays done in replicates ($n \geq 2$). Mean values are shown, and the standard deviations are <30% of the mean.

Table 3. HDAC Enzyme and Antiproliferative Activity Data for Spiropiperidine-*N*-hydroxyacrylamides 40, 44, 47, and 50^a

	R	HDAC	K562	A549	HCT-116
		(μM)	(μM)	(μM)	(μM)
40		1.21	2.95	5.25	2.33
44		1.19	3.27	4.70	3.51
47		9.02	38.6	≥ 50	28.2
50		5.15	>50	>50	32.8

^a Assays done in replicates ($n \geq 2$). Mean values are shown, and the standard deviations are <30% of the mean.

comprised *N*-hydroxy-{4-oxospiro[chromane-2,4'-piperidine]-6-yl}acrylamides with various *N*-piperidine substituents (22 and 30a–e). As summarized in Table 2, a remarkable potency increase was observed: the benzyl and the benzoyl analogues 30d and 30e with IC_{50} of 0.121 and 0.316 μM , respectively, were around 100 times more active than the corresponding *N*-hydroxy-spiro[chromane-2,4'-piperidine]-6-yl}carboxamides. A similar increase was found also for the methyl and the acetyl derivatives 30a and 30b, which showed potencies in the sub-micromolar range. Within the series no major differences in activities among the compounds were observed: compound 22 (R = H) with an IC_{50} of 0.082 μM was around 8-fold more active than the least potent one within this series, the acetyl analogue 30b. With the exception of 30b, all compounds of this subseries also showed good antiproliferative activity in the three cell lines in the micromolar or submicromolar range. The benzyl derivative 30d emerged as the most potent agent in two cell lines, with IC_{50} of 0.399 μM in K562 cells and 0.773 μM in the A549 cell line. The methyl analogue 30a was slightly more active in the HCT-116 cell line (IC_{50} = 0.266 μM) than the benzyl derivative (IC_{50} = 0.477 μM). Furthermore, the antiproliferative activity was in general slightly superior in the K562 and HCT-116 cell lines than in A549 cells.

The significant increase of activity of *N*-hydroxyacrylamide series compared to the *N*-hydroxybenzamide analogues prompted us to investigate further modifications of the spiro-piperidine scaffold: the first step was the synthesis of *N*-hydroxy-spiro[chromane-2,4'-piperidine]acrylamides, wherein the acrylamide moiety was shifted to position 7. As shown in Table 2, the benzoyl derivative 31e (IC_{50} = 0.366 μM) was essentially equipotent to 30e in the enzymatic assay, whereas the other four compounds of this series were 2- to 20-fold less active

compared to the spiro[chromane-2,4'-piperidine]-6-yl analogues. In addition, 23 (R = H), 31a (R = Me), and 31d (R = Bn) were about 10 times less potent in the three cell lines than the related analogues 22, 30a, and 30d. On the other hand, no major differences in the antiproliferative potencies were observed between the 7-spiropiperidines 31b, 31c, and 31e (IC_{50} in the low micromolar range) and the corresponding spiro[chromane-2,4'-piperidine]-6-yl analogues 30b, 30c, and 30e.

Subsequently, our attention was directed to *N*-substituted spirobenzofuran acrylhydroxamates. The enzymatic activity of the prepared analogues (Table 2, compounds 35 and 39a–e) was overall lower than the corresponding spiro[chromane-2,4'-piperidine]-6-yl derivatives. 35 with R = H (IC_{50} = 0.221 μM) was around 3 times less potent than the corresponding spirochromane analogue 22, and the methyl analogue 39a (IC_{50} = 0.538 μM) was 2 times less potent than the corresponding 30a. The decrease in the enzymatic activity was more evident in the cases of 39b, with R = acetyl (≥ 100 -fold), and 39c, with R = ethyloxycarbonyl (~ 20 -fold). With the exception of 35 and 39a, all other spirobenzofuran representatives were less potent than the corresponding spirochromanes in the cellular assays. Compounds 35 (R = H) and 39a (R = Me), with IC_{50} values in the submicromolar/low micromolar range in the three cell lines, had activity comparable to that of the corresponding spirochromane derivative 22 and 30a.

On the basis of the enzymatic and antiproliferative activities, the spiro[chromane-2,4'-piperidine]-6-yl series was selected for further exploration. Since the introduction of different *N*-substituents was well tolerated, our attention was directed toward the preparation of further different spiro-piperidines, in particular to assess the importance of the ketone moiety. In specific, analogues of the benzylspiro-piperidine analogue 30d were prepared

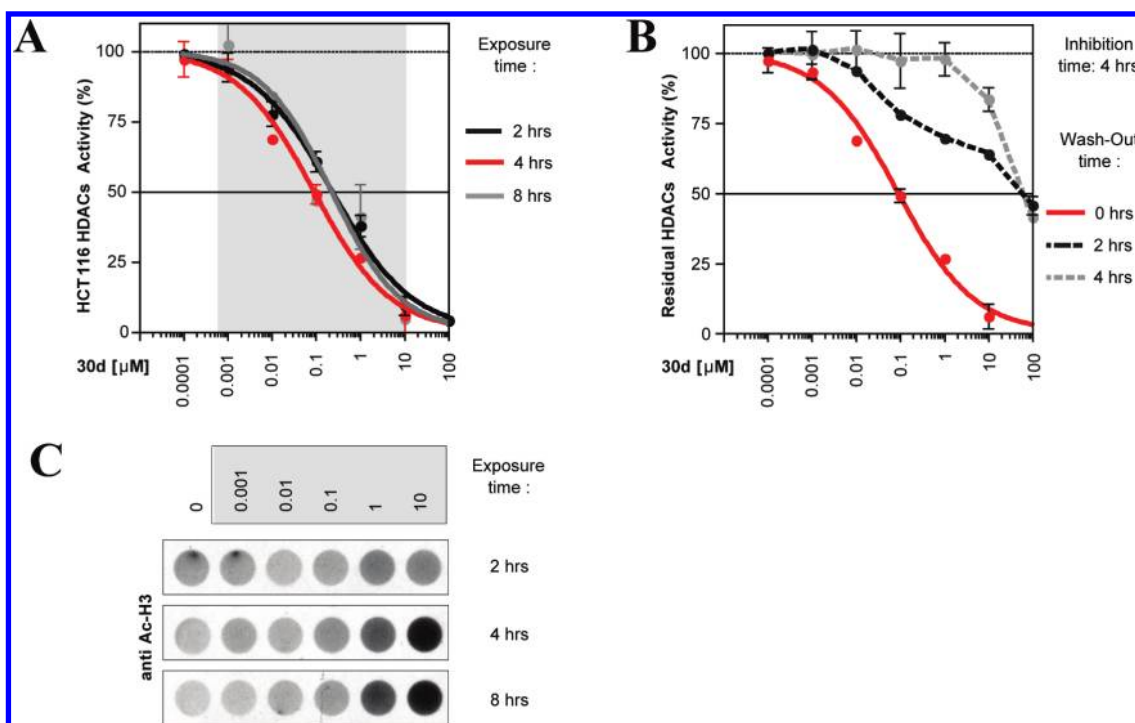


Figure 2. (A) Dose-dependent inhibition of whole-cell HDAC activity in cultured HCT-116 human colon cancer cells by **30d**. Cells were incubated with **30d** for 2, 4, or 8 h. (B) Whole-cell HDAC inhibitory activity of **30d** in HCT-116 cells in a washout experiment. Cells were treated with **30d** at various doses for 4 h. The inhibitor was then washed out with PBS, and fresh drug-free medium was added. The whole-cell HDAC activity was measured at the reported times. (C) Dose and time dependent induction of histone acetylation in HCT-116 human colon cancer cells after treatment with **30d**. Cells were incubated with **30d** for the reported times and concentrations before histone acetylation of the whole-cell lysates was analyzed by cyto blot.

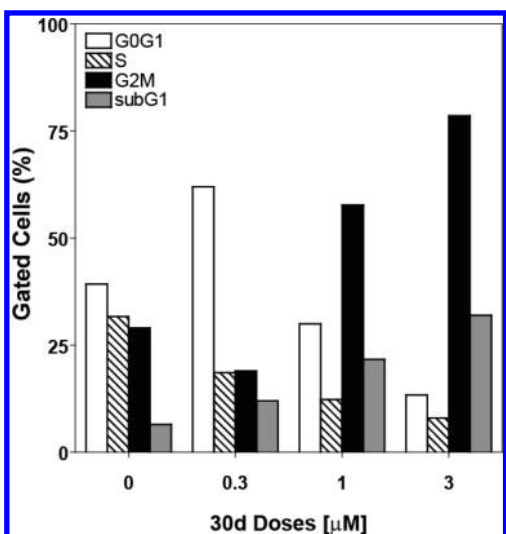


Figure 3. Cell cycle profiles of human cancer HCT-116 cells treated for 24 h with **30d** at different doses.

and tested; the hydroxy derivative **40** and the chromene **44** were around 10-fold less active than **30d** in the enzymatic assay. Furthermore, both compounds showed a lower antiproliferative activity in K562, A549, and HCT-116 cells. Also, the chromane **47** ($IC_{50} = 9.0 \mu M$) and the *N*-acetyl derivatives **50** ($IC_{50} = 5.15 \mu M$) showed a significantly reduced HDAC inhibitory activity and a substantially lower antiproliferative potency. These data demonstrate that the carbonyl group is critical for the biochemical and cellular potency of this series.

Table 4. Pharmacokinetic Properties of 30d in Mice

parameter	30d
$C_{max,iv}$ [μM]	12.5
$AUC_{iv,0-\infty}$ [ng h/mL]	847
$t_{1/2}$ [h]	8.4
Cl [(L/h)/kg]	5.88
V_{ss} [L/kg]	8.9
$C_{max,os}$ [μM]	0.823
t_{max} [h]	0.25
$AUC_{os,0-\infty}$ [ng h/mL]	800
F [%]	31.5

In summary, the benzyl derivative **30d** exhibited a good enzymatic and cellular potency, and thus, we selected it as a representative compound for a more extensive characterization. First, **30d** was submitted to Amphora Corp. (Research Triangle Park, NC, U.S.) to evaluate its inhibitory activity against HDACs 1, 3, 4, 6, and 8 subtypes. **30d** exhibited IC_{50} of 93.8, 9.4, 127, 25.7, and 1760 nM against HDACs 1, 3, 4, 6 and 8, respectively. This biological profile is typical for pan inhibitors, such as **1**, trichostatin A, and the previously published amidopropenyl hydroxamic acid derivatives.^{21,40,41}

On the basis of the biochemical inhibition data (using both human recombinant proteins and HeLa nuclear extracts as enzymatic sources), we investigated the enzymatic inhibitory activity of **30d** in intact human HCT-116 cancer cells in order to measure its whole-cell HDAC inhibitory activity.⁴² As shown in Figure 2A, **30d** exhibited a dose dependent inhibitory activity with an IC_{50} of around $0.1 \mu M$. These results are in good

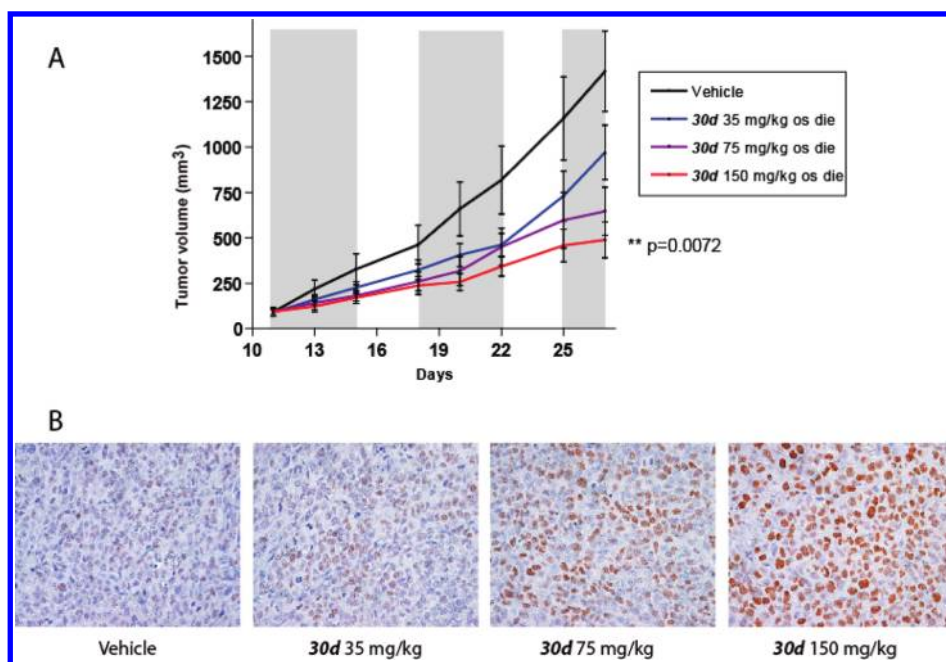


Figure 4. (A) Antitumor activity of **30d** against HCT-116 human tumor xenografts implanted in mice, expressed as mean tumor volume (expressed as $\text{mm}^3 \pm$ standard error of the mean (SEM)). (B) Analysis by immunohistochemistry of histone acetylation staining of the section of HCT-116 xenograft tumor at the end of treatment. Tumor sections were fixed in formalin, paraffin-embedded, and stained with an antibody recognizing acetylated histone H4. Representative sections of the staining for the different treatment groups are reported.

agreement with the biochemical data obtained using HeLa nuclear extract as the enzymatic source. Interestingly, the HDAC inhibitory activity was already maximal after 2 h of incubation. Moreover, **30d** completely inhibited the measurable enzymatic activity in HCT-116 cells, reaching the maximal plateau at $100 \mu\text{M}$.

The possible persistence of the inhibitory activity in whole cells was then evaluated in a drug washout experiment (Figure 2B). To this end, HCT-116 cells were exposed for 4 h at different concentrations of **30d** until complete inhibition of the HDAC enzymatic activity. Cells were then subsequently washed with drug-free media. As shown in Figure 2B, the inhibitory activity of **30d** was partially reversed and almost completely reversed after 2 and 4 h of drug washout.

Subsequently, a cybotlot assay dedicated to evaluate histone acetylation was carried out as further confirmation of the enzymatic inhibition and to define a temporal correlation between inhibition and its possible biological readout on well-known targets of HDAC inhibition (Figure 2C).⁴³ The experiments, which were performed at the same experimental conditions used for the whole cell HDAC inhibitory assay, underscored a dose and time dependent hyperacetylation of histone H3. The time dependency of histone hyperacetylation clearly indicated the presence of a lag time between the enzymatic inhibition, already maximal after 2 h of compound exposure, and biological readout, which was more evident after 4 h of exposure. Moreover, while the enzymatic inhibitory activity appeared to be already maximal after 2 h of exposure with no further increase after that time, the induced hyperacetylation of histones appeared to increase over the time of enzymatic inhibition.

Next, the cell cycle profile of the human cancer cell line HCT-116 treated with **30d** was analyzed by flow cytometry. As reported in the Figure 3, **30d** induced a strong increment of G0/G1 phase population, an associated decrease of S and G2/M population at the lowest dose, and an increase of G2M

population at both 1 and $3 \mu\text{M}$. A dose dependent increase of the subG1 population, an indication of cell death, was also noted.

Given the promising *in vitro* properties of spirocycle **30d**, we evaluated its *in vivo* behavior. Pharmacokinetic studies were carried out in male CD-1 mice, and the compound was administered in a single intravenous (iv) dose of 5 mg/kg or an oral dose of 15 mg/kg.²⁰ The main pharmacokinetic parameters obtained are reported in Table 4. The compound showed a systemic plasma clearance slightly greater than the hepatic blood flow of $5.4 (\text{mL/h})/\text{kg}$ in mice⁴⁴ but lower than the previously published clearance rates of the hydroxamic acid derivatives **1** ($6.73 (\text{mL/h})/\text{kg}$),^{45,20} **3** ($18.3 (\text{mL/h})/\text{kg}$),⁴⁵ and **4** ($11.6 (\text{mL/h})/\text{kg}$).⁴⁵ The estimated elimination half-life was 8.4 h, substantially higher than that of **1** (0.38 h), **3** (1.37 h), and **4** (1.21 h).^{45,20} The calculated steady state volume of distribution (8.9 L/kg) suggests an extensive tissue distribution. Moreover, the compound was quickly absorbed after oral administration with a t_{max} of 15 min and showed an oral bioavailability ($F = 31.5\%$) substantially higher than that of the three reference compounds **1**, **3**, and **4** (less than 10%).⁴⁵

The *in vivo* antitumor activity of spirocycle **30d** was then studied in an established human xenograft model obtained by implanted human colon carcinoma cells HCT-116 in athymic mice. Human cancer cells (HCT-116, 5×10^6) were injected subcutaneously in the flank of female CD-1 nude mice, and the treatment was initiated once the tumors reached a volume of around 100 mm^3 . The compound, dissolved in water containing 5% DMSO and 9.5% encapsin, was administered orally at 35–150 mg/kg for 5 days/week for 17 days. As shown in Figure 4A, the compound was able to reduce significantly the tumor volume in a dose dependent manner with respect to the control mice. Specifically, the calculated T/C ratio at the highest tested dose of 150 mg/kg was around 0.3, which was highly statistically significant ($p < 0.0072$). No significant body weight

differences among the groups of mice and no signs of overt toxicity were observed during the treatment. As previously described,²⁰ we had found that compound **1** at doses of 50 mg/kg was able to reduce, similarly to **30d**, the tumor growth in HCT-116 in athymic mice with a calculated *T/C* ratio of around 0.34 after 2 weeks of treatment. However, the compound was administered intraperitoneally once a day, which corresponds, to our best knowledge, to the optimal route of administration for compound **1** in these animal models.

Finally, tumor sections taken from mice treated with the vehicle or **30d** were analyzed by immunohistochemistry in order to establish a relationship between the antitumor activity observed in vivo in the xenograft model and HDAC inhibition. The histone acetylation level was followed as readout for HDAC inhibition.

As shown in the Figure 4B, the observed tumor response correlated well with a significant increase of histone acetylation level in the tumor section of groups treated with **30d** versus the vehicle group, in terms of both positive cells and signal intensity.

CONCLUSIONS

New spiro[chromane-2,4'-piperidine] and spiro[benzofuran-2,4'-piperidin] hydroxamic acid derivatives as HDAC inhibitors have been developed integrating a privileged structure with a hydroxamic acid moiety as zinc binding group. Four examples of *N*-hydroxy-spiro[chromane-2,4'-piperidine]-6-yl]carboxamides exhibited only a modest in vitro HDAC and cell growth inhibitory activity, but introduction of a *N*-hydroxyacrylamide group as zinc binding moiety led to a substantial increase in activity. The compounds exhibited IC₅₀ in the submicromolar range against HDACs and in the submicromolar to low micromolar range in the antiproliferative assay against three tumor cell lines. The synthesis of *N*-hydroxy[spiro(chromane-2,4'-piperidine)-7-yl]acrylamide analogues and the spirobenzofuran derivatives led to structures that were in general less active in the enzymatic and cellular assays. Furthermore, reduction, elimination, or general replacement of the carbonyl group of the spirochromane led to compounds with reduced potency. On the basis of the in vitro biochemical and antiproliferative activity, the spirocycle **30d** was selected for further in vitro and in vivo pharmacokinetic and activity experiments. Whole-cell HDAC inhibitory activity of **30d** was assessed in HCT-116 cells, and the cell cycle profiles of human cancer HCT-116 cells showed that the compound induced a strong increment of G0/G1 phase population at the lowest dose and an increase of G2M population at 1 and 3 μM. The compound, based on the good oral bioavailability (*F* = 31.5%) and its ability to inhibit tumor growth in a HCT-116 murine xenograft model in a dose dependent manner, was selected for further investigation.

EXPERIMENTAL SECTION

Chemistry. Reagents and solvents used, unless stated otherwise, were of commercially available reagent grade quality and were used without further purification. Flash chromatography purifications were performed on Merck silica gel 60 (0.04–0.063 mm). Nuclear magnetic resonance spectra (¹H NMR) were recorded on a Bruker 400 MHz spectrometer at 300 K and are referenced in ppm (δ) relative to TMS. Coupling constants (*J*) are expressed in hertz (Hz). HPLC–MS experiments were performed either on an Acquity UPLC apparatus, equipped with a diode array and a Micromass SQD single quadrupole (Waters) spectrometer or on an Agilent 1100, equipped with a diode

array and a Bruker ion trap Esquire 3000+. Purity was monitored at 254 nm, and the purities of the compounds used for biological tests were found to be at least 95% with the exception of **13c** (92%) and **22** (83%) (see Supporting Information).

***N*-Hydroxy-[1'-benzyl-4-oxospiro(chromane-2,4'-piperidine)-6-yl]carboxamide (13c).** A mixture of 3-acetyl-4-hydroxybenzoic acid methyl ester (8, 2.4 g, 12 mmol), *N*-BOC-piperidine-4-one (2.4 g, 12 mmol), and pyrrolidine (0.51 mL, 6.1 mmol) in MeOH (80 mL) was heated for 4 h at reflux. The solution was concentrated under vacuum and then poured into water. Then 1 M HCl was added until a neutral pH was obtained, and the product was extracted with AcOEt. The organic phase was dried over Na₂SO₄, filtered, and evaporated. The crude mixture was purified by silica gel chromatography (CH₂Cl₂/MeOH 97:3) to give the spirocycle **9** (1.45 g, 32%). ¹H NMR (CDCl₃) δ (ppm): 8.55 (d, *J* = 2.02 Hz, 1 H), 8.16 (dd, *J* = 8.74, 2.14 Hz, 1 H), 7.03 (d, *J* = 8.74 Hz, 1 H), 3.90 (s, 3 H), 3.25–3.19 (m, 2 H), 2.75 (s, 2 H), 2.46–2.43 (m, 2 H), 2.05–2.00 (m, 2 H), 1.67–1.59 (m, 2 H), 1.46 (s, 9 H). MS (ESI) *m/z*: 276 [M + H]⁺.

A 4 M solution of HCl in dioxane (10 mL) was added to a solution of compound **9** (1.4 g, 3.7 mmol) in CH₂Cl₂ (10 mL), and the mixture was stirred at room temperature for 4 h. The product was filtered off, washed with CH₂Cl₂, dried, and collected, giving the free amine **10** as its hydrochloride salt (1.03 g, 89%) as a white solid. ¹H NMR (DMSO-*d*₆) δ (ppm): 9.35 (bs, 1 H), 8.35 (d, *J* = 2.25 Hz, 1 H), 8.18 (dd, *J* = 8.71, 2.25 Hz, 1 H), 7.31 (d, *J* = 8.71 Hz, 1 H), 3.89 (s, 3 H), 3.25–3.15 (m, 4 H), 3.04 (s, 2 H), 2.14–2.18 (m, 2 H), 1.94–2.00 (m, 2 H). MS (ESI) *m/z*: 276 [M + H]⁺.

A suspension of the spirocycle **10** (250 mg, 0.80 mmol) in CH₂Cl₂ (10 mL) was treated with DIPEA (0.28 mL, 1.6 mmol) and benzyl bromide (95 μL, 0.80 mmol). After being stirred at room temperature for 2 h, the mixture was concentrated, and the crude residue was purified by column chromatography (CH₂Cl₂/MeOH 95:5) to give **11c** (275 mg, 94%) as a light yellow solid. ¹H NMR (CDCl₃) δ (ppm): 8.51 (d, *J* = 2.03 Hz, 1 H), 8.12 (dd, *J* = 8.76, 2.03 Hz, 1 H), 7.36–7.25 (m, 5 H), 7.02 (d, *J* = 8.76 Hz, 1 H), 4.56 (s, 2 H), 3.86 (s, 3 H), 2.73 (s, 2 H), 2.53–2.72 (m, 4 H), 2.04–2.06 (m, 2 H), 1.80–2.00 (m, 2 H). MS (ESI) *m/z*: 366 [M + H]⁺.

NaOH (60 mg, 1.5 mmol) in H₂O (4 mL) was added to a suspension of methyl ester **11c** (275 mg, 0.753 mmol) in MeOH (10 mL). The mixture was stirred at reflux for 1 h, then concentrated. The pH of the aqueous phase was adjusted with 1 M HCl to 5. The resulting suspension was extracted with CH₂Cl₂, the organic phase dried over Na₂SO₄ and concentrated to give the carboxylic acid **12c** (250 mg, 95%) as a white solid. ¹H NMR (DMSO-*d*₆) δ (ppm): 8.31 (bs, 1 H), 8.16–8.18 (m, 1 H), 7.60–7.70 (m, 2 H), 7.40–7.50 (m, 3 H), 7.21–7.23 (m, 1 H), 4.40 (s, 2 H), 3.17–3.22 (m, 4 H), 2.93 (s, 2 H), 2.09–2.22 (m, 4 H). MS (ESI) *m/z*: 352 [M + H]⁺.

A solution of compound **12c** (250 mg, 0.712 mmol) in CH₂Cl₂ (20 mL) was cooled to 0 °C. EDC (203 mg, 1.06 mmol) and HOBT (143 mg, 1.06 mmol) were added, and the mixture was stirred at room temperature for 3 h. NH₂OTHP (100 mg, 0.85 mmol) in CH₂Cl₂ (1 mL) was added dropwise, and the solution was stirred at room temperature overnight. The reaction mixture was then washed with saturated NaHCO₃ and brine, dried over Na₂SO₄, and concentrated. The crude residue was purified by silica gel chromatography (CH₂Cl₂/MeOH 95:5) to give [1'-benzyl-4-oxospiro(chromane-2,4'-piperidine)-6-yl]-*N*-(tetrahydro-pyran-2-yloxy)amide (85 mg, 26%). ¹H NMR (CDCl₃) δ (ppm): 8.18 (d, *J* = 2.30 Hz, 1 H), 8.01 (dd, *J* = 8.82, 2.49 Hz, 1 H), 7.26–7.31 (m, 5 H), 7.04 (d, *J* = 8.82 Hz, 1 H), 5.07 (s, 1 H), 3.97–4.02 (m, 1 H), 3.62–3.64 (m, 1 H), 3.54 (s, 2 H), 2.72 (s, 2 H), 2.61–2.63 (m, 2 H), 2.41–2.46 (m, 2 H), 1.81–2.00 (m, 10 H). MS (ESI) *m/z*: 451 [M + H]⁺. Then 1 M HCl in Et₂O (5 mL) was added dropwise to a solution of the THP hydroxamate (79.8 mg, 0.177 mmol) in CH₂Cl₂ (5 mL). The precipitating solid was filtered

off, washed with CH_2Cl_2 , and dried giving the requisite hydroxamic acid **13c** as a light yellow solid (55 mg, 80%). ^1H NMR ($\text{DMSO}-d_6$) δ (ppm): 10.52 (bs, 1 H), 9.05 (bs, 1 H), 8.23 (s, 1 H), 8.06–8.08 (m, 1 H), 7.63–7.64 (m, 2 H), 7.51 (s, 3 H), 7.20–7.21 (m, 1 H), 4.41 (s, 2 H), 3.23–3.36 (m, 4 H), 2.96 (s, 2 H), 2.08–2.24 (m, 4 H). MS (ESI) m/z : 367 $[\text{M} + \text{H}]^+$.

(E)-N-Hydroxy-3-{4-oxospiro[chromane-2,4'-piperidine]-6-yl}acrylamide (22). A mixture of 2-hydroxy-5-bromoacetophenone (**14**, 10.7 g, 50.0 mmol), *N*-BOC-piperidin-4-one (9.96 g, 50.0 mmol), and pyrrolidine (2.1 mL, 25 mmol) in MeOH (80 mL) was heated to reflux for 11 h. The solvent was then removed, and the crude mixture was purified by column chromatography (hexane/AcOEt 9:1 to 8:2) to give the spirocycle **16** as a yellow solid (18.55 g, 94%). ^1H NMR (CDCl_3) δ (ppm): 7.96 (s, 1 H), 7.55 (d, $J = 8.8$ Hz, 1 H), 6.82 (d, $J = 7.6$ Hz, 1 H), 3.83–3.86 (m, 2 H), 3.18 (t, $J = 11.6$ Hz, 2 H), 2.70 (s, 2 H), 1.98–2.01 (m, 2 H), 1.58–1.62 (m, 2 H), 1.44 (s, 9 H). MS (ESI) m/z : 420 $[\text{M} + \text{Na}]^+$.

A mixture of compound **16** (1.04 g, 2.62 mmol), $\text{Pd}(\text{OAc})_2$ (59 mg, 0.26 mmol), PPh_3 (137 mg, 0.522 mmol), TEA (0.73 mL, 5.2 mmol), methyl acrylate (0.47 mL, 5.2 mmol) in dry DMF (10 mL) was heated at 100 °C for 8 h. The mixture was cooled to room temperature, filtered on a Celite pad, and washed with AcOEt (100 mL). The filtrate was washed with NH_4Cl , saturated NaHCO_3 , and brine. The organic phase was dried over Na_2SO_4 and evaporated under vacuum. The crude residue was purified by column chromatography (hexane/AcOEt 9:1 to 7:3) to give the acrylic acid methyl ester **18** as a light yellow solid (594 mg, 56%). ^1H NMR (CDCl_3) δ (ppm): 8.00 (bs, 1 H), 7.60–7.65 (m, 2 H), 7.00 (d, $J = 8.4$ Hz, 1 H), 6.31 (d, $J = 16.0$ Hz, 1 H), 3.85 (bs, 2 H), 3.78 (s, 3 H), 3.20 (t, $J = 12.0$ Hz, 2 H), 2.73 (s, 2 H), 2.00 (d, $J = 15.2$ Hz, 2 H), 1.53–1.70 (m, 2 H), 1.44 (s, 9 H). MS (ESI) m/z : 424 $[\text{M} + \text{Na}]^+$.

NaOH (160 mg, 4.00 mmol) in H_2O (2 mL) was added to a suspension of methyl ester **18** (462 mg, 1.15 mmol) in MeOH (6 mL), and the mixture was stirred at 50 °C. After 2 h, MeOH was evaporated and the pH of the aqueous phase was adjusted to 5 with 1 M HCl. The resulting suspension was extracted with CH_2Cl_2 , the organic phase dried over Na_2SO_4 and concentrated to give the carboxylic acid **20** as a white solid (410 mg, 92%). ^1H NMR (CDCl_3) δ (ppm): 8.05 (d, $J = 2.0$ Hz, 1 H), 7.68–7.74 (m, 2 H), 7.04 (d, $J = 8.8$ Hz, 1 H), 6.39 (d, $J = 16.0$ Hz, 1 H), 3.85–3.94 (m, 2 H), 3.19–3.25 (m, 2 H), 2.75 (s, 2 H), 1.59–1.68 (m, 4 H), 1.50 (s, 9 H). MS (ESI) m/z : 410 $[\text{M} + \text{Na}]^+$.

A solution of the acrylic acid **20** (387 mg, 1.00 mmol) in CH_2Cl_2 (15 mL) was cooled to 0 °C. EDC (383 mg, 2.00 mmol) and HOBt (135 mg, 1.00 mmol) were added, and the mixture was stirred at room temperature for 1 h. NH_2OTHP (146 mg, 1.25 mmol) in CH_2Cl_2 (1 mL) was added dropwise, and the mixture was stirred at room temperature for 4 h. Then the solution was washed with saturated NaHCO_3 and brine, dried over Na_2SO_4 , and concentrated. The crude residue was purified by silica gel chromatography ($\text{CH}_2\text{Cl}_2/\text{MeOH}$ 98:2) to give *(E)*-3-{1'-*tert*-butoxycarbonyl-4-oxospiro[chromane-2,4'-piperidine]-6-yl}-*N*-(tetrahydropyran-2-yloxy)acrylamide as a light yellow oil (464 mg, 95%). ^1H NMR ($\text{DMSO}-d_6$) δ (ppm): 7.91 (s, 1 H), 7.80 (d, $J = 7.6$ Hz, 1 H), 7.48 (d, $J = 16.0$ Hz, 1 H), 7.14 (d, $J = 8.4$ Hz, 1 H), 6.46 (d, $J = 16.0$ Hz, 1 H), 4.90 (bs, 1 H), 3.84–3.90 (m, 1 H), 3.70–3.77 (m, 2 H), 3.52–3.55 (m, 1 H), 3.10–3.16 (m, 2 H), 2.88 (s, 2 H), 1.81–1.90 (m, 4 H), 1.53–1.70 (m, 6 H), 1.40 (s, 9 H). MS (ESI) m/z : 995.7 $[\text{M} + \text{Na}]^+$. Then 4 M HCl in dioxane (2 mL) was added dropwise to a solution of the *N*-(tetrahydropyran-2-yloxy)acrylamide intermediate (434 mg, 0.892 mmol) in CH_2Cl_2 (10 mL) and the mixture was stirred at room temperature for 2 h. The precipitate was filtered off, washed with CH_2Cl_2 , and dried to give the desired hydroxamic acid **22** as a white solid (260 mg, 86%, hydrochloride salt). ^1H NMR ($\text{DMSO}-d_6$) δ (ppm): 10.27 (bs, 1 H), 8.98 (bs, 1 H), 7.90 (d, $J = 2.0$ Hz, 1 H), 7.81 (dd, $J = 8.8, 2.4$ Hz, 1 H), 7.44 (d, $J = 16.0$ Hz,

1 H), 7.19 (d, $J = 8.4$ Hz, 1 H), 6.45 (d, $J = 16.0$ Hz, 1 H), 3.06–3.19 (m, 4 H), 2.95 (s, 2 H), 2.10–2.14 (m, 2 H), 1.89–1.93 (m, 2 H). MS (ESI) m/z : 627 $[\text{M} + \text{Na}]^+$.

(E)-N-Hydroxy-3-{1'-benzyl-4-oxospiro[chromane-2,4'-piperidine]-6-yl}acrylamide (30d). A 4 M solution of HCl in dioxane (4 mL) was added to compound **18** (1.18 g, 2.94 mmol) in CH_2Cl_2 (20 mL), and the mixture was stirred at room temperature for 4 h. The precipitated solid was filtered off, washed with CH_2Cl_2 , then dried under vacuum to give **24** as a white solid (748 mg, 77%, hydrochloride salt). ^1H NMR ($\text{DMSO}-d_6$) δ (ppm): 8.95 (bs, 2 H), 8.01–8.06 (m, 2 H), 7.69 (d, $J = 16.0$ Hz, 1 H), 7.20 (d, $J = 7.2$ Hz, 1 H), 6.60 (d, $J = 16.0$ Hz, 1 H), 3.72 (s, 3 H), 3.17–3.21 (m, 2 H), 3.07–3.13 (m, 2 H), 2.99 (s, 2 H), 2.08–2.13 (m, 2 H), 1.88–1.95 (m, 2 H). MS (ESI) m/z : 302 $[\text{M} + \text{H}]^+$.

A suspension of compound **24** (451 mg, 1.34 mmol) in CH_2Cl_2 (12 mL) was treated with TEA (0.42 mL, 3.0 mmol) and benzyl bromide (0.54 mL, 4.5 mmol), and the mixture was stirred at room temperature for 5 h. The mixture was washed with water, and the pH value was adjusted to 5 with 0.5 M HCl. The organic phase was dried, concentrated, and the crude residue was purified by silica gel chromatography ($\text{CH}_2\text{Cl}_2/\text{MeOH}$ 95:5) to give the spirocycle **26d** as a light yellow solid (440 mg, 84%). ^1H NMR (CDCl_3) δ (ppm): 8.02 (d, $J = 2.0$ Hz, 1 H), 7.61–7.67 (m, 2 H), 7.51–7.57 (m, 2 H), 7.47–7.50 (m, 3 H), 7.01 (d, $J = 9.2$ Hz, 1 H), 6.38 (d, $J = 16.0$ Hz, 1 H), 3.80 (s, 3 H), 3.51–3.58 (m, 2 H), 2.74–2.77 (m, 2 H), 2.60–2.64 (m, 2 H), 2.45–2.47 (m, 2 H), 2.03–2.05 (m, 2 H), 1.73–1.80 (m, 2 H), 1.52–1.59 (m, 2 H). MS (ESI) m/z : 805.5 $[\text{M} + \text{Na}]^+$.

Hydrolysis of the methyl ester **26d** (414 mg, 1.06 mmol) was performed as described for **20**, giving the carboxylic acid **28d** as a white solid (380 mg, 96%). ^1H NMR (CDCl_3) δ (ppm): 8.02 (d, $J = 2.0$ Hz, 1 H), 7.64–7.68 (m, 2 H), 7.44–7.49 (m, 5 H), 7.01 (d, $J = 9.2$ Hz, 1 H), 6.38 (d, $J = 16.0$ Hz, 1 H), 3.62–3.70 (m, 2 H), 3.15–3.22 (m, 2 H), 2.68–2.77 (m, 4 H), 2.35–2.44 (m, 2 H), 1.99–2.08 (m, 2 H). MS (ESI) m/z : 378 $[\text{M} + \text{H}]^+$.

Reaction of the acrylic acid **28d** (365 mg, 0.967 mmol) with NH_2OTHP was carried out following the procedure for compound **22**. The crude THP intermediate was purified by column chromatography ($\text{CH}_2\text{Cl}_2/\text{MeOH}$ 97:3) (328 mg, 69%). ^1H NMR (CDCl_3) δ (ppm): 8.31 (bs, 1 H), 8.05 (d, $J = 2.0$ Hz, 1 H), 7.54–7.68 (m, 2 H), 7.32–7.40 (m, 4 H), 6.96–6.98 (m, 1 H), 6.36 (bs, 1 H), 4.99 (bs, 1 H), 3.93–3.97 (m, 1 H), 3.68–3.66 (m, 1 H), 3.45–3.54 (m, 1 H), 2.76 (s, 2 H), 2.63–2.66 (m, 2 H), 2.40–2.50 (m, 2 H), 2.04–2.12 (m, 2 H), 1.81–1.84 (m, 4 H), 1.51–1.60 (m, 6 H). MS (ESI) m/z : 477 $[\text{M} + \text{H}]^+$. Deprotection of tetrahydropyranyl group gave the requisite hydroxamic acid **30d** as a light yellow solid (230 mg, 78%, hydrochloride salt). ^1H NMR ($\text{DMSO}-d_6$) δ (ppm): 10.69 (bs, 1 H), 7.91 (d, $J = 2.0$ Hz, 1 H), 7.84 (dd, $J = 8.6, 1.9$ Hz, 1 H), 7.55–7.69 (m, 2 H), 7.36–7.54 (m, 4 H), 7.15 (d, $J = 8.5$ Hz, 1 H), 6.45 (d, $J = 15.8$ Hz, 1 H), 4.37 (d, $J = 5.2$ Hz, 2 H), 3.06–3.34 (m, 4 H), 2.88 (s, 2 H), 1.97–2.25 (m, 4 H). MS (ESI) m/z : 393 $[\text{M} + \text{H}]^+$.

(E)-N-Hydroxy-3-{1'-benzyl-4-hydroxyspiro[chromane-2,4'-piperidine]-6-yl}acrylamide (40). A mixture of the hydroxamic acid **30d** (60 mg, 0.14 mmol) and NaBH_4 (18 mg, 0.48 mmol) in MeOH (5 mL) was stirred at room temperature. After 3 h the solution was evaporated and the crude residue was purified by preparative HPLC to give the hydroxy derivative **40** (45 mg, 58%, trifluoroacetate). ^1H NMR ($\text{DMSO}-d_6$) δ (ppm): 10.64 (bs, 1 H), 9.60 (bs, 1 H), 7.36–7.63 (m, 8 H), 6.89 (d, $J = 8.52$ Hz, 1 H), 6.30 (d, $J = 16.0$ Hz, 1 H), 4.71 (bs, 1 H), 4.39 (s, 2 H), 3.25–3.29 (m, 6 H), 2.18–1.81 (m, 4 H). MS (ESI) m/z : 395 $[\text{M} + \text{H}]^+$.

Biological Assays. *Pan-HDAC Inhibition Assay.* Pan-HDAC inhibition assays were performed as previously described.²⁰

HDACs 1, 3, 4, 6, and 8 Inhibition Assay. The inhibition assays for HDACs 1, 3, 4, 6, and 8 were carried out by Amphora Discovery Corp.

(Research Triangle Park, NC, U.S.) as previously described.^{41,40} Purified HDACs were incubated with the test compounds and a carboxyfluorescein-labeled peptide (1 μ M) as substrate for 17 h at 25 °C in a buffer consisting of 100 mM HEPES (pH 7.5), 1 mg/mL BSA, 0.01% Triton X-100, 1% DMSO, and 25 mM KCl. The reaction was stopped by addition of 45 μ L of 100 mM HEPES (pH 7.5) and 0.08% sodium dodecyl sulfate, and the substrate and the product were then separated electrophoretically using a LabChip 3000 system (Caliper Life Sciences, Hopkinton, MA) with blue laser excitation and green fluorescence detection. All experiments were performed in duplicate. IC₅₀ values were determined from 12-point concentration–response curves using a nonlinear regression analysis.

HDAC Whole-Cell Assay. HCT-116 cells were seeded into 96-well plates (Corning Inc., Costar) at a density of 2×10^4 cells/well in a volume of 50 μ L of the appropriate tissue culture medium. Compounds were added with different concentrations for the indicated incubation time at 37 °C with 5% CO₂. KI-104 Fluor de Lys substrate was then added to initiate the reaction (final concentration of 500 μ M). The reaction was stopped at the reported times, and fluorescence was developed by adding 50 μ L of a freshly prepared stop mix, which is composed of the Fluor-de-Lys developer diluted at 1:60 (BIOMOL), 1 μ M TSA (BIOMOL), and 1% NP40. Substrate fluorescence was measured using an excitation at 355 nm and an emission at 460 nm after 10 min of reaction.

Cell Growth Assay. The antiproliferative effect of the HDAC inhibitors on cell proliferation was evaluated against K562 (chronic myeloid carcinoma), A549 (non-small-cell lung cancer), and HCT-116 (human colon cancer) tumor cell lines using the CellTiter-Glo luminescent cell viability assay (Promega, Madison, WI) according to the manufacturer's instructions. K562, A549, and HCT-116 cells, in exponential growth, were incubated for 72 h at different concentrations of the inhibitors. Then an equivalent of the CellTiter-Glo reagent was added, the solution was mixed for 2 min in order to induce cell lysis, and the luminescence was recorded after a further 10 min. The IC₅₀ was calculated using GraphPad software.

Flow Cytometric Cell Cycle Analysis. Cells were treated with **30d** for 24 h, then harvested and fixed with 70% ethanol at –20 °C. Nucleic acids from fixed cells were treated with RNase type IIIA (1 mg/mL) and stained with propidium iodide (50 mg/mL). DNA content was measured by using a fluorescence-activated cell cytometer (FACScan, Becton Dickinson, Franklin Lakes, NJ) and analyzed using CellQuest Pro software.

Cytoblot Assay. HCT-116 cells were seeded at the density of 2×10^4 per well and allowed to attach overnight at 37 °C with 5% CO₂. **30d** was added at the reported doses and for the indicated times. Then the cells were fixed with 100% methanol at –20 °C for 10 min, washed twice in Tris-buffered saline buffer containing 0.1% Triton X-100 (TBST), and finally blocked with 5% milk in TBST buffer. The hyperacetylation was determined using an antibody recognizing acetylated histone H3 (Upstate 06599), diluted 1:200 in 5% milk in TBST, after incubation overnight at 4 °C.

In Vivo Drug Pharmacokinetic and Efficacy Experiments. In vivo pharmacokinetic in mice and efficacy experiments in a human HCT-116 xenograft model in mice were performed as previously described.²⁰ The T/C ratio corresponds to the mean relative tumor volume of the treated tumors/mean relative volume of control group. Analysis was performed using *t* test statistics (two tailed). The iv formulation for the pharmacokinetic experiments comprised 2% DMSO and 9.8% encapsin in water. For oral dosing the inhibitor was dissolved in water containing 5% DMSO and 9.5% encapsin.

Immunohistochemistry (IHC) of Tumor Xenografts. Tumor xenografts were recovered 2 h after the last compound administration and fixed in formalin. Formalin-fixed and paraffin-embedded tumors were stained for histone H4 acetylation: the xenograft tissue sections were

deparaffinized, rehydrated, unmasked using TEG buffer (10 mM Tris + 0.5 mM EGTA, pH 9), and treated for 5 min with 3% H₂O₂. Slides were then incubated overnight at 4 °C with an antibody against acetylated histone H4,⁴⁶ revealed using the EnVision Plus/HRP detection system (Dako), and counterstained with hematoxylin.

■ ASSOCIATED CONTENT

S Supporting Information. Synthesis and characterization of compounds **13a,b,d**, **23**, **30a–c,e**, **31a–e**, **35**, **39a–e**, **44**, **47**, and **50**; purity of key compounds as determined by HPLC. This material is available free of charge via the Internet at <http://pubs.acs.org>.

■ AUTHOR INFORMATION

Corresponding Author

*Phone: +390294375130. Fax: +390294375138. E-mail: florian.thaler@ifom-ieo-campus.it.

■ ACKNOWLEDGMENT

The authors are grateful to Dr. Raffaella Amici, Dr. Stefania Gagliardi, Dr. Andrea Colombo, and Dr. Simon Plyte for their helpful discussions and the critical review of the manuscript.

■ ABBREVIATIONS USED

HDAC, histone deacetylases; HAT, histone acetyltransferases; K562, chronic myelogenous leukemia cell line; A549, carcinomic human alveolar basal epithelial cells; HCT-116, human colorectal carcinoma cell line; BSA, bovine serum albumin; IHC, immunohistochemistry; PK, pharmacokinetics; TBST, Tris-buffered saline and Triton X-100

■ REFERENCES

- (1) Hong, L.; Schroth, G. P.; Matthews, H. R.; Yau, P.; Bradbury, E. M. Studies of the DNA binding properties of histone H4 amino terminus. Thermal denaturation studies reveal that acetylation markedly reduces the binding constant of the H4 “tail” to DNA. *J. Biol. Chem.* **1993**, *268*, 305–314.
- (2) Selvi, R. B.; Kundu, T. K. Reversible acetylation of chromatin: implication in regulation of gene expression, disease and therapeutics. *Biotechnol. J.* **2009**, *4*, 375–390.
- (3) de Ruijter, A. J.; van Gennip, A. H.; Caron, H. N.; Kemp, S.; van Kuilenburg, A. B. Histone deacetylases (HDACs): characterization of the classical HDAC family. *Biochem. J.* **2003**, *370*, 737–749.
- (4) Haberland, M.; Montgomery, R. L.; Olson, E. N. The many roles of histone deacetylases in development and physiology: implications for disease and therapy. *Nat. Rev. Genet.* **2009**, *10*, 32–42.
- (5) Minucci, S.; Pelicci, P. G. Histone deacetylase inhibitors and the promise of epigenetic (and more) treatments for cancer. *Nat. Rev. Cancer* **2006**, *6*, 38–51.
- (6) Glozak, M. A.; Seto, E. Histone deacetylases and cancer. *Oncogene* **2007**, *26*, 5420–5432.
- (7) Spange, S.; Wagner, T.; Heinzl, T.; Kramer, O. H. Acetylation of non-histone proteins modulates cellular signalling at multiple levels. *Int. J. Biochem. Cell Biol.* **2009**, *41*, 185–198.
- (8) Paris, M.; Porcelloni, M.; Binaschi, M.; Fattori, D. Histone deacetylase inhibitors: from bench to clinic. *J. Med. Chem.* **2008**, *51*, 1505–1529.
- (9) Carey, N.; La Thangue, N. B. Histone deacetylase inhibitors: gathering pace. *Curr. Opin. Pharmacol.* **2006**, *6*, 369–375.

- (10) Rasheed, W.; Bishton, M.; Johnstone, R. W.; Prince, H. M. Histone deacetylase inhibitors in lymphoma and solid malignancies. *Expert Rev. Anticancer Ther.* **2008**, *8*, 413–432.
- (11) Khan, O.; La Thangue, N. B. Drug insight: histone deacetylase inhibitor-based therapies for cutaneous T-cell lymphomas. *Nat. Clin. Pract. Oncol.* **2008**, *5*, 714–726.
- (12) Marks, P. A. Discovery and development of SAHA as an anticancer agent. *Oncogene* **2007**, *26*, 1351–1356.
- (13) Marks, P. A.; Breslow, R. Dimethyl sulfoxide to vorinostat: development of this histone deacetylase inhibitor as an anticancer drug. *Nat. Biotechnol.* **2007**, *25*, 84–90.
- (14) Bates, S. E.; Zhan, Z.; Steadman, K.; Obrzut, T.; Luchenko, V.; Frye, R.; Robey, R. W.; Turner, M.; Gardner, E. R.; Figg, W. D.; Steinberg, S. M.; Ling, A.; Fojo, T.; To, K. W.; Piekarczyk, R. L. Laboratory correlates for a phase II trial of romidepsin in cutaneous and peripheral T-cell lymphoma. *Br. J. Haematol.* **2010**, *148*, 256–267.
- (15) Atadja, P. Development of the pan-DAC inhibitor panobinostat (LBH589): successes and challenges. *Cancer Lett.* **2009**, *280*, 233–41.
- (16) Steele, N. L.; Plumb, J. A.; Vidal, L.; Tjornelund, J.; Knoblauch, P.; Rasmussen, A.; Ooi, C. E.; Buhl-Jensen, P.; Brown, R.; Evans, T. R.; DeBono, J. S. A phase I pharmacokinetic and pharmacodynamic study of the histone deacetylase inhibitor belinostat in patients with advanced solid tumors. *Clin. Cancer Res.* **2008**, *14*, 804–810.
- (17) Novotny-Diermayr, V.; Sangthongpitag, K.; Hu, C. Y.; Wu, X.; Sausgruber, N.; Yeo, P.; Greicius, G.; Pettersson, S.; Liang, A. L.; Loh, Y. K.; Bonday, Z.; Goh, K. C.; Hentze, H.; Hart, S.; Wang, H.; Ethirajulu, K.; Wood, J. M. SB939, a novel potent and orally active histone deacetylase inhibitor with high tumor exposure and efficacy in mouse models of colorectal cancer. *Mol. Cancer Ther.* **2010**, *9*, 642–652.
- (18) Gojo, I.; Jiemjit, A.; Trepel, J. B.; Sparreboom, A.; Figg, W. D.; Rollins, S.; Tidwell, M. L.; Greer, J.; Chung, E. J.; Lee, M. J.; Gore, S. D.; Sausville, E. A.; Zwiebel, J.; Karp, J. E. Phase I and pharmacologic study of MS-275, a histone deacetylase inhibitor, in adults with refractory and relapsed acute leukemias. *Blood* **2007**, *109*, 2781–2790.
- (19) Zhou, N.; Moradei, O.; Raepel, S.; Leit, S.; Frechette, S.; Gaudette, F.; Paquin, I.; Bernstein, N.; Bouchain, G.; Vaisburg, A.; Jin, Z.; Gillespie, J.; Wang, J.; Fournel, M.; Yan, P. T.; Trachy-Bourget, M. C.; Kalita, A.; Lu, A.; Rahil, J.; MacLeod, A. R.; Li, Z.; Besterman, J. M.; Delorme, D. Discovery of *N*-(2-aminophenyl)-4-[(4-pyridin-3-ylpyrimidin-2-ylamino)methyl]benzamide (MGCD0103), an orally active histone deacetylase inhibitor. *J. Med. Chem.* **2008**, *51*, 4072–4075.
- (20) Thaler, F.; Colombo, A.; Mai, A.; Amici, R.; Bigogno, C.; Boggio, R.; Cappa, A.; Carrara, S.; Cataudella, T.; Fusar, F.; Gianti, E.; Joppolo di Ventimiglia, S.; Moroni, M.; Munari, D.; Pain, G.; Regalia, N.; Sartori, L.; Vultaggio, S.; Dondio, G.; Gagliardi, S.; Minucci, S.; Mercurio, C.; Varasi, M. Synthesis and biological evaluation of *N*-hydroxyphenyl-acrylamides and *N*-hydroxypyridin-2-yl-acrylamides as novel histone deacetylase inhibitors. *J. Med. Chem.* **2010**, *53*, 822–829.
- (21) Thaler, F.; Colombo, A.; Mai, A.; Bigogno, C.; Boggio, R.; Carrara, S.; Joppolo di Ventimiglia, S.; Munari, D.; Regalia, N.; Dondio, G.; Gagliardi, S.; Minucci, S.; Mercurio, C.; Varasi, M. Synthesis and biological characterization of amidopropenyl-hydroxamates as HDAC inhibitors. *ChemMedChem* **2010**, *5*, 1359–1372.
- (22) DeSimone, R. W.; Currie, K. S.; Mitchell, S. A.; Darrow, J. W.; Pippin, D. A. Privileged structures: applications in drug discovery. *Comb. Chem. High Throughput Screening* **2004**, *7*, 473–494.
- (23) Costantino, L.; Barlocco, D. Privileged structures as leads in medicinal chemistry. *Curr. Med. Chem.* **2006**, *13*, 65–85.
- (24) Beghyn, T.; Deprez-Poulain, R.; Willand, N.; Folleas, B.; Deprez, B. Natural compounds: leads or ideas? Bioinspired molecules for drug discovery. *Chem. Biol. Drug Des.* **2008**, *72*, 3–15.
- (25) Evans, B. E.; Rittle, K. E.; Bock, M. G.; DiPardo, R. M.; Freidinger, R. M.; Whitter, W. L.; Lundell, G. F.; Veber, D. F.; Anderson, P. S.; Chang, R. S.; et al. Methods for drug discovery: development of potent, selective, orally effective cholecystokinin antagonists. *J. Med. Chem.* **1988**, *31*, 2235–2246.
- (26) Elliott, J. M.; Selnick, H. G.; Claremon, D. A.; Baldwin, J. J.; Buhrow, S. A.; Butcher, J. W.; Habecker, C. N.; King, S. W.; Lynch, J. J., Jr.; Phillips, B. T.; et al. 4-Oxospiro[benzopyran-2,4'-piperidines] as class III antiarrhythmic agents. Pharmacological studies on 3,4-dihydro-1'-[2-(benzofurazan-5-yl)-ethyl]-6-methanesulfonamidospiro[(2*H*)-1-benzopyran-2,4'-piperidin]-4-one (L-691,121). *J. Med. Chem.* **1992**, *35*, 3973–3976.
- (27) Nerenberg, J. B.; Erb, J. M.; Bergman, J. M.; O'Malley, S.; Chang, R. S.; Scott, A. L.; Broten, T. P.; Bock, M. G. 4-Oxospiro[benzopyran-2,4'-piperidines] as selective alpha 1a-adrenergic receptor antagonists. *Bioorg. Med. Chem. Lett.* **1999**, *9*, 291–294.
- (28) Yamato, M.; Hashigaki, K.; Tsutsumi, A.; Tasaka, K. Synthesis and structure–activity relationship of spiro[isochroman-piperidine] analogs for inhibition of histamine release. II. *Chem. Pharm. Bull. (Tokyo)* **1981**, *29*, 3494–3498.
- (29) Yang, L.; Morriello, G.; Prendergast, K.; Cheng, K.; Jacks, T.; Chan, W. W.; Schleim, K. D.; Smith, R. G.; Patchett, A. A. Potent 3-spiropiperidine growth hormone secretagogues. *Bioorg. Med. Chem. Lett.* **1998**, *8*, 107–112.
- (30) Harsanyi, K.; Szabadkai, I.; Borza, I.; Karpati, E.; Kiss, B.; Pellionisz, M.; Farkas, S.; Horvath, C.; Csomor, K.; Lapis, E.; Laszlovszky, I.; Szabo, S.; Kis-Varga, A.; Laszy, J.; Gere, A. Novel Spiro [2*H*-1-Benzopyran-2, 4'-piperidine]-4(3*H*)-one Derivatives, and Addition Salts Thereof and Pharmaceutical Compositions Containing Them. WO97/37630, 1997.
- (31) Le Bourdonnec, B.; Windh, R. T.; Ajello, C. W.; Leister, L. K.; Gu, M.; Chu, G. H.; Tuthill, P. A.; Barker, W. M.; Koblisch, M.; Wiant, D. D.; Graczyk, T. M.; Belanger, S.; Cassel, J. A.; Feschenko, M. S.; Brogdon, B. L.; Smith, S. A.; Christ, D. D.; Derelanko, M. J.; Kutz, S.; Little, P. J.; DeHaven, R. N.; DeHaven-Hudkins, D. L.; Dolle, R. E. Potent, orally bioavailable delta opioid receptor agonists for the treatment of pain: discovery of *N,N*-diethyl-4-(5-hydroxyspiro[chromene-2,4'-piperidine]-4-yl)benzamide (ADLS859). *J. Med. Chem.* **2008**, *51*, 5893–5896.
- (32) Le Bourdonnec, B.; Windh, R. T.; Leister, L. K.; Zhou, Q. J.; Ajello, C. W.; Gu, M.; Chu, G. H.; Tuthill, P. A.; Barker, W. M.; Koblisch, M.; Wiant, D. D.; Graczyk, T. M.; Belanger, S.; Cassel, J. A.; Feschenko, M. S.; Brogdon, B. L.; Smith, S. A.; Derelanko, M. J.; Kutz, S.; Little, P. J.; DeHaven, R. N.; DeHaven-Hudkins, D. L.; Dolle, R. E. Spirocyclic delta opioid receptor agonists for the treatment of pain: discovery of *N,N*-diethyl-3-hydroxy-4-(spiro[chromene-2,4'-piperidine]-4-yl) benzamide (ADLS747). *J. Med. Chem.* **2009**, *52*, 5685–5702.
- (33) Uto, Y.; Ueno, Y.; Kiyotsuka, Y.; Miyazawa, Y.; Kurata, H.; Ogata, T.; Yamada, M.; Deguchi, T.; Konishi, M.; Takagi, T.; Wakimoto, S.; Ohsumi, J. Synthesis and evaluation of novel stearyl-CoA desaturase 1 inhibitors: 1'-{6-[5-(pyridin-3-ylmethyl)-1,3,4-oxadiazol-2-yl]pyridazin-3-yl}-3,4-dihydrospiro[chromene-2,4'-piperidine] analogs. *Eur. J. Med. Chem.* **2010**, *45*, 4788–4796.
- (34) Uto, Y.; Kiyotsuka, Y.; Ueno, Y.; Miyazawa, Y.; Kurata, H.; Ogata, T.; Deguchi, T.; Yamada, M.; Watanabe, N.; Konishi, M.; Kurikawa, N.; Takagi, T.; Wakimoto, S.; Kono, K.; Ohsumi, J. Novel spiro-piperidine-based stearyl-CoA desaturase-1 inhibitors: identification of 1'-{6-[5-(pyridin-3-ylmethyl)-1,3,4-oxadiazol-2-yl]pyridazin-3-yl}-5-(trifluoromethyl)-3,4-dihydrospiro[chromene-2,4'-piperidine]. *Bioorg. Med. Chem. Lett.* **2010**, *20*, 746–754.
- (35) Shinde, P.; Srivastava, S. K.; Odedara, R.; Tuli, D.; Munshi, S.; Patel, J.; Zambad, S. P.; Sonawane, R.; Gupta, R. C.; Chauthaiwale, V.; Dutt, C. Synthesis of spiro[chroman-2,4'-piperidin]-4-one derivatives as acetyl-CoA carboxylase inhibitors. *Bioorg. Med. Chem. Lett.* **2009**, *19*, 949–953.
- (36) Reiser, U.; Kraemer, O.; Sennhenn, P.; Spevak, W. Spiro-(thio) Benzopyran-2,4'-piperidine- and Cyclohexane Derivatives as Inhibitors of Specific Cell Cycle Enzyme. WO2007/128782, 2007.
- (37) Cochran, J. E.; Wu, T.; Padwa, A. Synthesis of polysubstituted anilines using the Diels–Alder reaction of methyl 5-aminofuroate. *Tetrahedron Lett.* **1996**, *37*, 2903–2906.
- (38) Klymchenko, A. S.; Mély, Y. 7-(2-Methoxycarbonylvinyl)-3-hydroxychromones: new dyes with red shifted dual emission. *Tetrahedron Lett.* **2004**, *45*, 8391–8394.
- (39) Wilson, R. A.; Chan, L.; Wood, R.; Brown, R. C. Synthesis and derivatisation of a novel spiro[1-benzofuran-2,4'-piperidin]-3-one scaffold. *Org. Biomol. Chem.* **2005**, *3*, 3228–3235.

(40) Blackwell, L.; Norris, J.; Suto, C. M.; Janzen, W. P. The use of diversity profiling to characterize chemical modulators of the histone deacetylases. *Life Sci.* **2008**, *82*, 1050–1058.

(41) Kozikowski, A. P.; Chen, Y.; Gaysin, A.; Chen, B.; D'Annibale, M. A.; Suto, C. M.; Langley, B. C. Functional differences in epigenetic modulators—superiority of mercaptoacetamide-based histone deacetylase inhibitors relative to hydroxamates in cortical neuron neuroprotection studies. *J. Med. Chem.* **2007**, *50*, 3054–3061.

(42) Fournel, M.; Bonfils, C.; Hou, Y.; Yan, P. T.; Trachy-Bourget, M. C.; Kalita, A.; Liu, J.; Lu, A. H.; Zhou, N. Z.; Robert, M. F.; Gillespie, J.; Wang, J. J.; Ste-Croix, H.; Rahil, J.; Lefebvre, S.; Moradei, O.; Delorme, D.; Macleod, A. R.; Besterman, J. M.; Li, Z. MGCD0103, a novel isotype-selective histone deacetylase inhibitor, has broad spectrum antitumor activity in vitro and in vivo. *Mol. Cancer Ther.* **2008**, *7*, 759–768.

(43) Haggarty, S. J.; Koeller, K. M.; Wong, J. C.; Grozinger, C. M.; Schreiber, S. L. Domain-selective small-molecule inhibitor of histone deacetylase 6 (HDAC6)-mediated tubulin deacetylation. *Proc. Natl. Acad. Sci. U.S.A.* **2003**, *100*, 4389–4394.

(44) Davies, B.; Morris, T. Physiological parameters in laboratory animals and humans. *Pharm. Res.* **1993**, *10*, 1093–1095.

(45) Yeo, P.; Xin, L.; Goh, E.; New, L. S.; Zeng, P.; Wu, X.; Venkatesh, P.; Kantharaj, E. Development and validation of high-performance liquid chromatography–tandem mass spectrometry assay for 6-(3-benzoyl-ureido)-hexanoic acid hydroxyamide, a novel HDAC inhibitor, in mouse plasma for pharmacokinetic studies. *Biomed. Chromatogr.* **2007**, *21*, 184–189.

(46) Ronzoni, S.; Faretta, M.; Ballarini, M.; Pelicci, P.; Minucci, S. New method to detect histone acetylation levels by flow cytometry. *Cytometry, Part A* **2005**, *66*, 52–61.